Matrix Biology Plus 24 (2024) 100163

Contents lists available at ScienceDirect

Matrix Biology Plus

journal homepage: www.sciencedirect.com/journal/matrix-biology-plus

Bone quality relies on hyaluronan synthesis – Insights from mice with complete knockout of hyaluronan synthase expression

A. Saalbach [a,1], M. Stein [b,1], S. Lee [b], U. Krügel [c], M. Haffner-Luntzer [d], K. Krohn [e], S. Franz [a], J.C. Simon [a], J. Tuckermann [b], U. Anderegg [a,*]

[a] Dept. of Dermatology, Venereology and Allergology, Medical Faculty, Leipzig University, Germany
[b] Institute of Comparative Molecular Endocrinology (CME), Ulm University, Germany
[c] Rudolf Boehm Institute of Pharmacology and Toxicology, Medical Faculty, Leipzig University, Germany
[d] Institute of Orthopaedic Research and Biomechanics, University Medical Center Ulm, Ulm, Germany
[e] Core Unit DNA Technologies, Leipzig University, Germany

ARTICLE INFO

Keywords:
Hyaluronan synthase
Bone
Osteogenic differentiation

ABSTRACT

Bone consists of a complex mineralised matrix that is maintained by a controlled equilibrium of synthesis and resorption by different cell types. Hyaluronan (HA) is an important glycosaminoglycan in many tissues including bone.

Previously, the importance of HA synthesis for bone development during embryogenesis has been shown. We therefore investigated whether HA synthesis is involved in adult bone turnover and whether abrogation of HA synthesis in adult mice would alter bone quality.

To achieve complete abrogation of HA synthesis in adult mice, we generated a novel Has-total knockout (Has-tKO) mouse model in which a constitutive knockout of Has1 and Has3 was combined with an inducible, Ubc-Cre-driven Has2 knockout.

By comparing bone tissue from wild-type, Has1,3 double knockout and Has-tKO mice, we demonstrate that Has2-derived HA mainly contributes to the HA content in bone. Furthermore, Has-tKO mice show a significant decrease of bone integrity in trabecular and cortical bone, as shown by μ-CT analysis. These effects are detectable as early as five weeks after induced Has2 deletion, irrespective of sex and progress with age.

Mesenchymal stem cells (MSC) during osteogenic differentiation *in vitro* showed that Has2 expression is increased while Has3 expression is decreased during differentiation. Furthermore, the complete abrogation of HA synthesis results in significantly reduced osteogenic differentiation as indicated by reduced marker gene expression (Runx-2, Tnalp, Osterix) as well as alizarin red staining. RNAseq analysis revealed that MSC from Has-tKO are characterised by decreased expression of genes annotated for bone and organ development, whereas expression of genes associated with chemokine related interactions and cytokine signalling is increased.

Taken together, we present a novel mouse model with complete deletion of HA synthases in adult mice which has the potential to study HA function in different organs and during age-related HA reduction. With respect to bone, HA synthesis is important for maintaining bone integrity, presumably based on the strong effect of HA on osteogenic differentiation.

Introduction

Bone represents a mineralized connective tissue with a complex extracellular matrix. The tissue undergoes a permanent turnover in adults when it is resorbed by osteoclasts and re-synthesized by osteoblasts. Osteocytes are known to orchestrate this process thus ensuring

Abbreviations: HA, hyaluronan; Has, HA synthase; Hyal, hyaluronidase; KO, knockout; HMW-HA, high-molecular-weight-HA; LMW, low- molecular-weight-HA; UbC, ubiquitin C; MSC, mesenchymal stem cells.

* Corresponding author at: Dept. of Dermatology, Venereology and Allergology, Leipzig University, Medical Faculty Max-Bürger-Forschungszentrum, Johannisallee 30, 04103 Leipzig, Germany.
E-mail address: Ulf.Anderegg@medizin.uni-leipzig.de (U. Anderegg).

[1] These authors contributed equally.

https://doi.org/10.1016/j.mbplus.2024.100163
Received 15 August 2024; Received in revised form 30 September 2024; Accepted 2 October 2024
Available online 9 October 2024

the functionality of the tissue [1].

Bone matrix is secreted by osteoblasts, their main matrix products are collagen type I (90 % collagenous proteins), osteocalcin, osteonectin, fibronectin, bone sialoprotein I/II, and proteoglycans (decorin, biglycan and lumican). Subsequently, this provisional matrix mineralizes when Ca^{2+} and phosphate ions form hydroxyapatite crystals [1]. A large fraction of murine bone is formed by endochondral ossification where a cartilagenous scaffold is converted into bone by osteoblasts.

Hyaluronan (HA) is a high molecular weight, linear, non-sulfated polymer of a disaccharide of glucuronic acid and N-Acetylglucosamine and is a major component of the cartilage. HA is a major part of the extracellular matrix of many organs with highest amounts in skin and cartilage. In bones, HA was detected in the maturational and hypertrophic zones of cartilages, the regional areas of the periosteum and endosteum (around osteoblasts, osteoprogenitor cells, and osteoclasts), osteocyte lacunae, and surrounding blood vessels [2]. HA is crucial during embryonic development enabling cell migration and differentiation [3]. Importantly in cartilage, the interaction of HA with aggrecan and link proteins enables the unique swelling capacities of the functional tissue [4]. In mineralized bone, earlier studies suggest that HA is involved in pre-osteoblast recruitment, proliferation and differentiation plus osteocyte crosstalk (reviewed in [5]).

HA is synthesized by three HA synthases (Has1, Has2 and Has3) which are located at the cell membrane [6,7]. Unlike many other proteoglycans, HA is extruded into the extracellular space without further modification during synthesis. There, HA can bind directly to cellular receptors (e.g. CD44, Lyve-1) and form a protective pericellular coat [8]. In addition, HA can form complex structures with other proteins and proteoglycans within the ECM (reviewed in [9,10]). The three Has enzymes show distinct expression profiles, with Has2 being the most active in many cells and tissues including cartilage and chondrocytes [11]. *In vitro*, both osteoblasts and osteoclasts can be a source of HA as shown in various models reviewed in [5].

In mice, a global, constitutive knockout (KO) of the most active synthase, Has2, is embryonically lethal due to failures in heart development [3]. Both conditional overexpression and conditional knockout of Has2 severely perturb skeletal growth, chondrocyte maturation and synovial joint formation [12–14]. During embryonic growth, chondrocyte-derived HA is essential, as mice with Has2 deficient chondrocytes exhibit perinatal lethality and severe skeletal dysfunctions [12]. These include dwarfism, bone shortage, extensive mineralisation in the diaphysis, and a disorganized growth plate region with reduced matrix content. The authors suggested that, in embryos, the cartilage *anlagen* are not affected by Has2 knockout, but the cartilage remodelling by chondrocytes is severely impaired and may not be compensated by residual Has1 or Has3 [12]. *In vitro* analyses have shown that embryonic osteoblast differentiation is acutely sensitive to HA levels and is strongly regulated in a time-resolved manner [15].

Has1 and Has3 are less important for organismal development, as mice with constitutive knockout of Has1 and Has3 or both are viable, breed and grow normally. However, these mice show a mild phenotype in terms of bone mineralisation and strength [16]. In addition, compensation of Has1,3 knockout by increased Has2 expression has been reported in the skin of such Has1,3 knockout mice [17].

Apart from its known role in bone development, the impact of HA synthesis on bone maintenance in the adult organism has not been addressed. We developed a novel mouse strain with inducible, ubiquitinC-cre driven knockout of the Has2 promoter ($Has2^{loxp/loxp}$-UbC-$cre^{ERT+/-}$) on the background of a constitutive double knockout of Has1 and Has3 (Has1,3-DKO; kindly provided by Prof. E. Maytin, Cleveland) [17]. The resulting $Has1,3^{-/-}$ $Has2^{loxp/loxp}$-UbC-$cre^{ERT+/-}$mice lack expression of all known HA synthases (*Has-tKO*) upon tamoxifen-induced recombination. This mouse model will be used to study the impact of a strong HA reduction in the adult organism, as it is thought to be a suitable model to study the age-related decrease in HA synthesis that affects many organs, including bone [18].

To demonstrate the functionality of the ubiquitin promoter in this model, we analysed HA levels in different organs of Has-tKO mice and performed a phenotyping of the mice in terms of motility and energy expenditure. Detailed analyses of bone quality following induction of the total Has KO were performed in comparison to wild-type and Has1,3-DKO animals. Finally, we investigated the effect of abrogated HA synthesis on the osteogenic differentiation capacity of bone marrow-derived mesenchymal stem cells (MSC) *in vitro* and compared the transcriptomes of differentiating MSC from wild-type and Has-tKO mice.

Results

To get an overview of the HA content in different organs, organs from adult wild-type mice were collected and the HA content per mg wet organ weight was determined. As expected, whole skin and serum contain by far the highest amounts of HA. Tibiae contain moderate amounts of HA (30–111 ng/mg, mean 66.9 ng/mg), as do aorta, brain, eye, heart and lung. Liver, kidney and spleen were found to contain the lowest amounts of HA (2–10 ng/mg) (Fig. 1A).

Hyaluronan is strongly decreased in serum, bones and other organs in Has-tKO mice

The effect of constitutive knockout of Has1,3 and additional induced KO of Has2 on organ HA levels was analysed by ELISA in different tissues (Fig. 1B). While the absence of Has1 and Has3 reduces HA levels in different tissues to varying degrees, the additional induced knockout of Has2 in the Has-tKO mice had a superior HA-reducing effect in all organs analysed. There were no gender-specific differences detectable in all cohorts used (not shown).

As previous studies have shown an impact of HA on bone development, we investigated the consequences of the knockdown HA synthesis on bone in adult animals. RT-qPCR analysis of bones from wildtype mice indicates that Has2 mRNA is highest and Has3 is expressed at comparable order of magnitude in whole bone tissue, while Has1 is only marginally expressed. In the knockout mice, the detectable Has-mRNA levels in the bone tissue follow the prediction of our genetic models (Fig. 2). While Has1 and Has 3 are not detectable in the KO animals, Has2 expression is substantially decreased in the bone after tamoxifen induction showing that bone tissue is also accessible to inducible Cre-recombination. Since the expression of the main hyaluronidases was not modified or altered (Supplemental Fig. 1), HA content is decreased probably exclusively by abrogation of HA synthesis.

Has-knockout does not affect activity, heat production and respiratory exchange rate (RER) in adult mice

As we have generated a new model with proposed modifications of the extracellular matrix that could affect the functionality of certain tissues, phenotyping was carried out in particular with regard to motility and energy consumption, since HA synthesis is an energy-consuming process, as it needs active glucose- and glutamine-utilizing pathways for the biosynthesis of its precursors N-acetyl-D-glucosamine (GlcNAc) and D-glucuronic acid (GlcUA) [19,20]. Initial observations revealed no visible differences in animals' behaviour within their home cages. A more detailed analysis was performed by examining the mice in the PhenoMaster® metabolic screening platform. In summary, no abnormalities of Has-tKO, even in long-lasting triple KO, were detectable (Supplemental Fig. 2).

Loss of HA synthesis attenuates bone quality in adult mice

Having established an adequate reduction of Has in our mouse models, the bone integrity upon induction of total Has knockout in adult mice of different ages was compared with Has1,3-DKO and wild-type animals. Micro-CT analysis revealed decreased trabecular and cortical

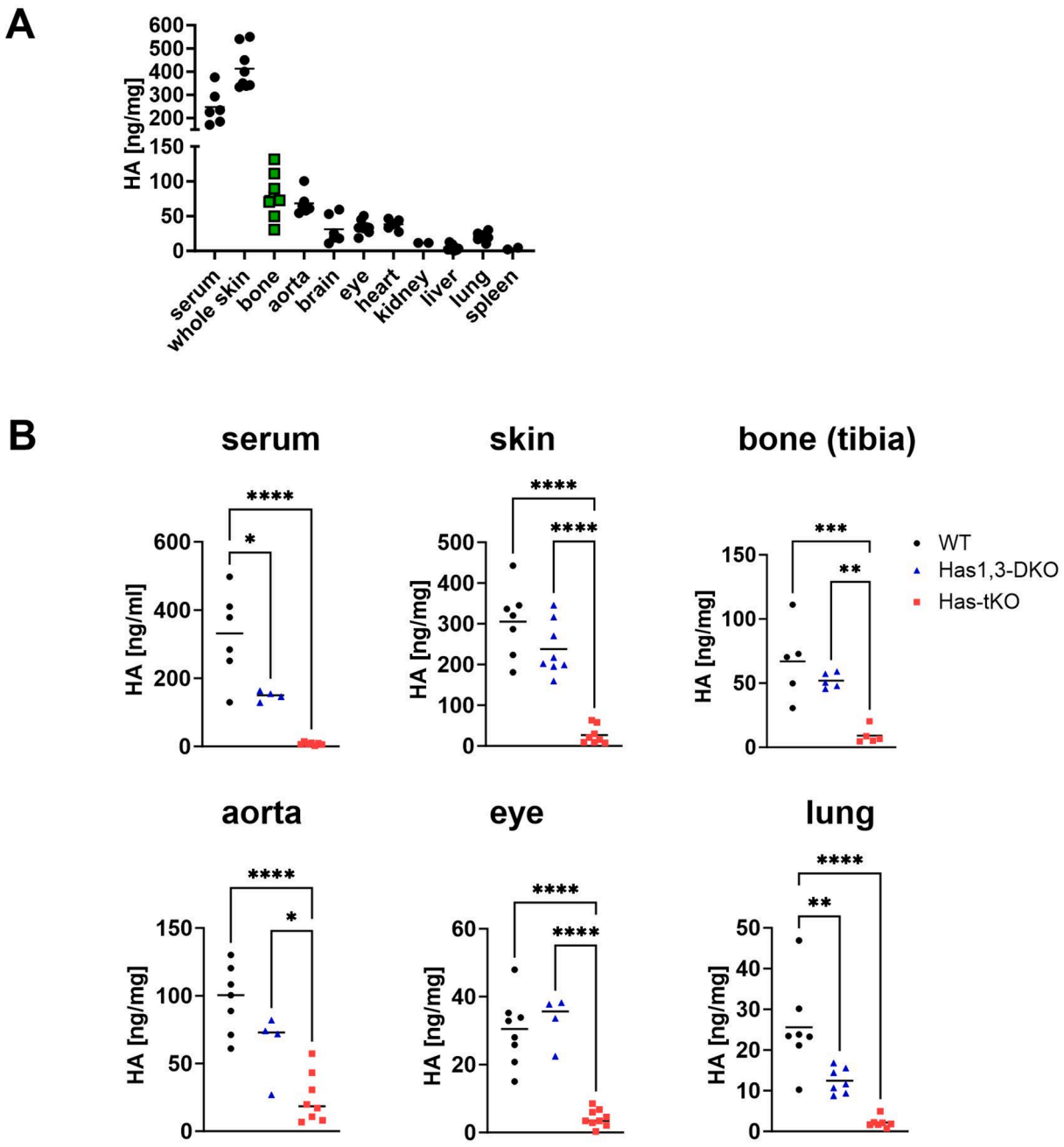

Fig. 1. Organ distribution of HA and impact of Has knockout. (A) HA content varies in different organs of adult mice. HA was measured by ELISA after enzymatic tissue dissociation and calculated per mg of tissue weight. (B) Knockout of HA synthases reduces HA concentration in different organs. HA content was detected in the indicated organs of wild-type (WT) mice, mice with a constitutive double KO of Has1 and Has3 (Has1,3-DKO) and mice with an induced complete KO of all Has (Has-tKO). Mice of both sexes were treated with tamoxifen at 8–10 weeks and used at 15–25 weeks of age. Each point represents one mouse. ANOVA with Tukey's multiple comparison test *$p < 0.05$, **$p < 0.005$, ***$p < 0.001$, ****$p < 0.0001$.

bone when HA synthesis was reduced for five weeks (Fig. 3) with different degrees in Has1,3-DKO and Has-tKO mice.

MicroCT analysis of trabecular bones demonstrated a mild decrease in bone volume per tissue volume and the number of trabeculae upon constitutive knockout of Has1 and Has3 (Has1,3-DKO). These effects were drastically increased upon additional, induced knockout of Has2 (Has-tKO) and affected all parameters of the morphometric analysis including bone volume, surface, trabecular thickness and separation (Fig. 3A,C).

The structure of cortical bone in the femur of Has-tKO mice was also impaired as indicated by increased bone surface per volume, enhanced bone porosity and reduced cortical bone cross sectional thickness (Fig. 3B,D). Comparing the different mouse strains, we found that the induced knockout of Has2 had much stronger effects on the quality of cortical bone than the constitutive knockout of Has1,3 in the littermates (Fig. 3B). However, the loss of HA did not change the bone mineral density measured by Calcium hydroxyapatite content of the bones (Fig. 3D).

The biomechanical strength of those femurs from wildtype and Has-tKO mice was investigated in bending experiments in order to identify the impact of strong HA-loss on bone stiffness. A strong reduction of HA synthesis resulted in a significant decrease of bending stiffness of the femurs (Supplemental Fig. 3).

Based on this strong phenotype of impaired bone quality in adult

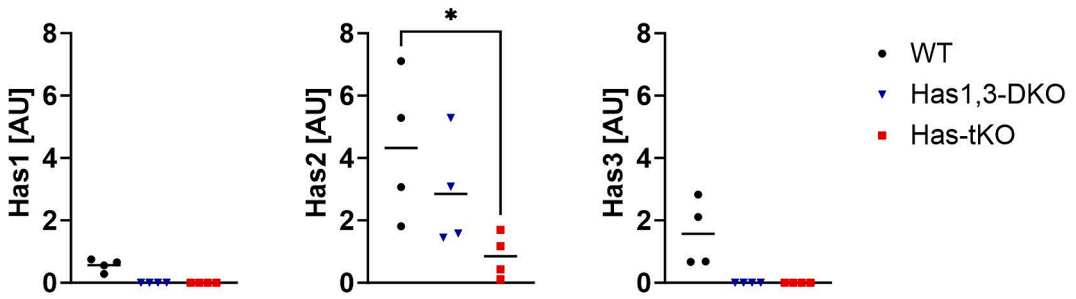

Fig. 2. Knockout of Has-enzymes is reflected by strongly reduced Has mRNA expression in bones of adult mice. RT-qPCR from bone tissue from adult female mice after tamoxifen treatment. Has1 mRNA was not detectable in bone tissue from Has1,3-DKO and Has-tKO mice. One-way ANOVA, * $p < 0.05$.

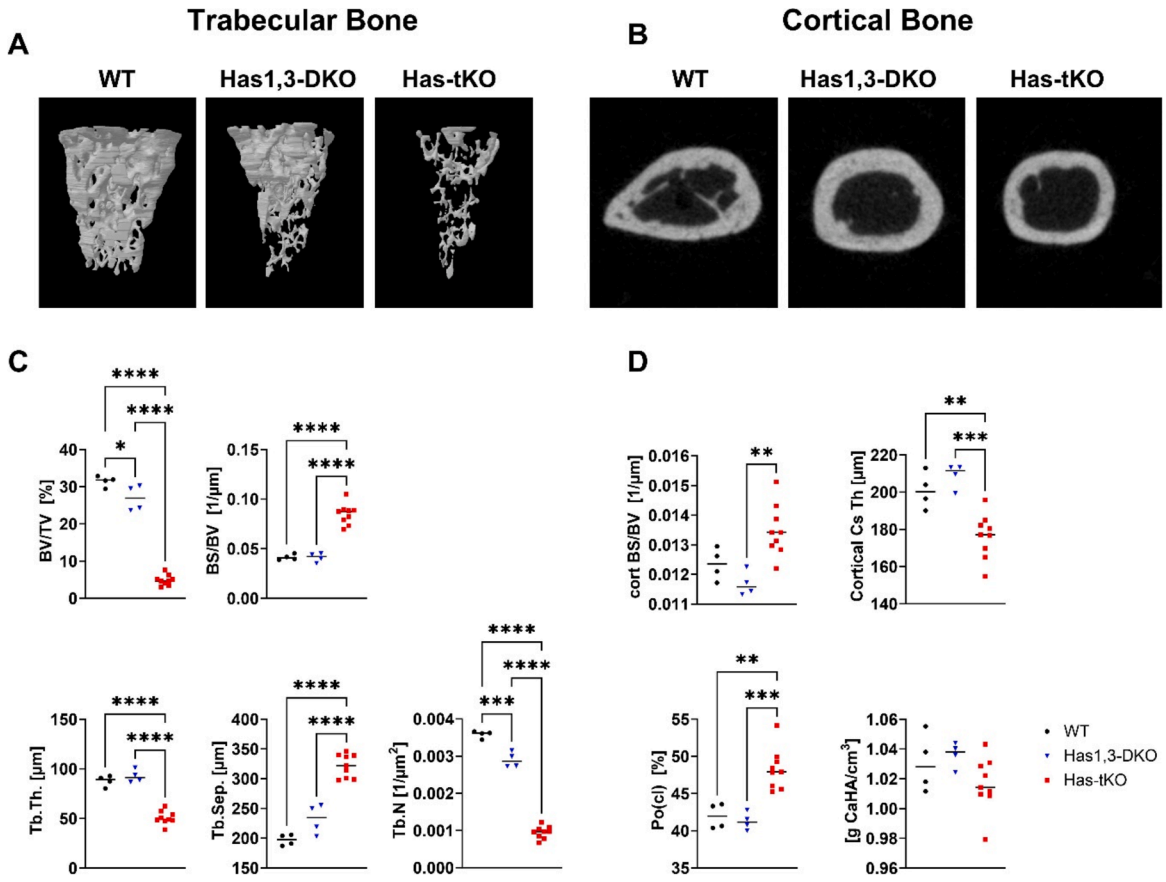

Fig. 3. Knockout of HA synthases leads to impaired bone quality as detected by µCT analysis of adult mouse femurs. Images of bone material loss in (A) trabecular and (B) cortical bone of femurs in male Has1,3-DKO and Has-tKO mice. (C) Quantitation of bone volume/total volume (BV/TV), bone surface/bone volume (BS/BV), trabecular thickness (Tb.Th.), separation (Tb.Sep.) and number (Tb.N) in trabecular bones. (D) Quantitation of bone surface/bone volume, cortical cross-sectional thickness (Cs.Th.), closed porosity (Po(cl)) and cortical bone density. Femurs were obtained for µCT analysis from a cohort of adult male mice treated with tamoxifen at 8–10 weeks of age. C57Bl6 mice were treated in the same way and used as wild-type controls. Ordinary one-way ANOVA, * $p < 0.05$, *** $p < 0.0005$, **** $p < 0.0001$.

male mice just five weeks after induction of the Has2 knockout we asked whether this phenotype might progress with age and can be observed in females as well. To address this question, we analysed two cohorts of female wild-type and Has-tKO mice. The younger cohort consisted of females at 25 weeks of age that had received tamoxifen 15–16 weeks earlier. The second cohort were females from wildtype and Has-tKO mice at 61 weeks of age that had lost Has2 expression for 53 weeks. First, similar to male mice (Fig. 3), younger female mice show significant bone loss in the trabecular and cortical bone of the femur upon complete Has knockout (Fig. 4). Next, the trabecular bones of younger Has-tKO mice were similar to trabecular bones of the older wild-type mice at 61 weeks of age in terms of bone surface to volume and bone volume to tissue volume ratios (Fig. 4, Supplemental Table 1). Similarly, the Has-tKO-derived femurs had a reduced number of trabeculae and thinner trabecular bone at younger ages, comparable to aged wild-types (Supplemental Table 1). With age, the trabecular bones of both genotypes showed signs of progressive bone loss as evidenced by the numbers of trabeculae, their thickness and separation. Furthermore, the significant differences between the genotypes persisted at older ages (Fig. 4, Supplemental Table 1). In the cortical bone, the bone surface to volume, cortical thickness and bone porosity showed significant age-related changes with significantly impaired cortical bone values for the Has-tKO mice. Thus, the bone phenotype of abrogated HA synthesis can be observed in both sexes and progresses with age (Fig. 4, Supplemental

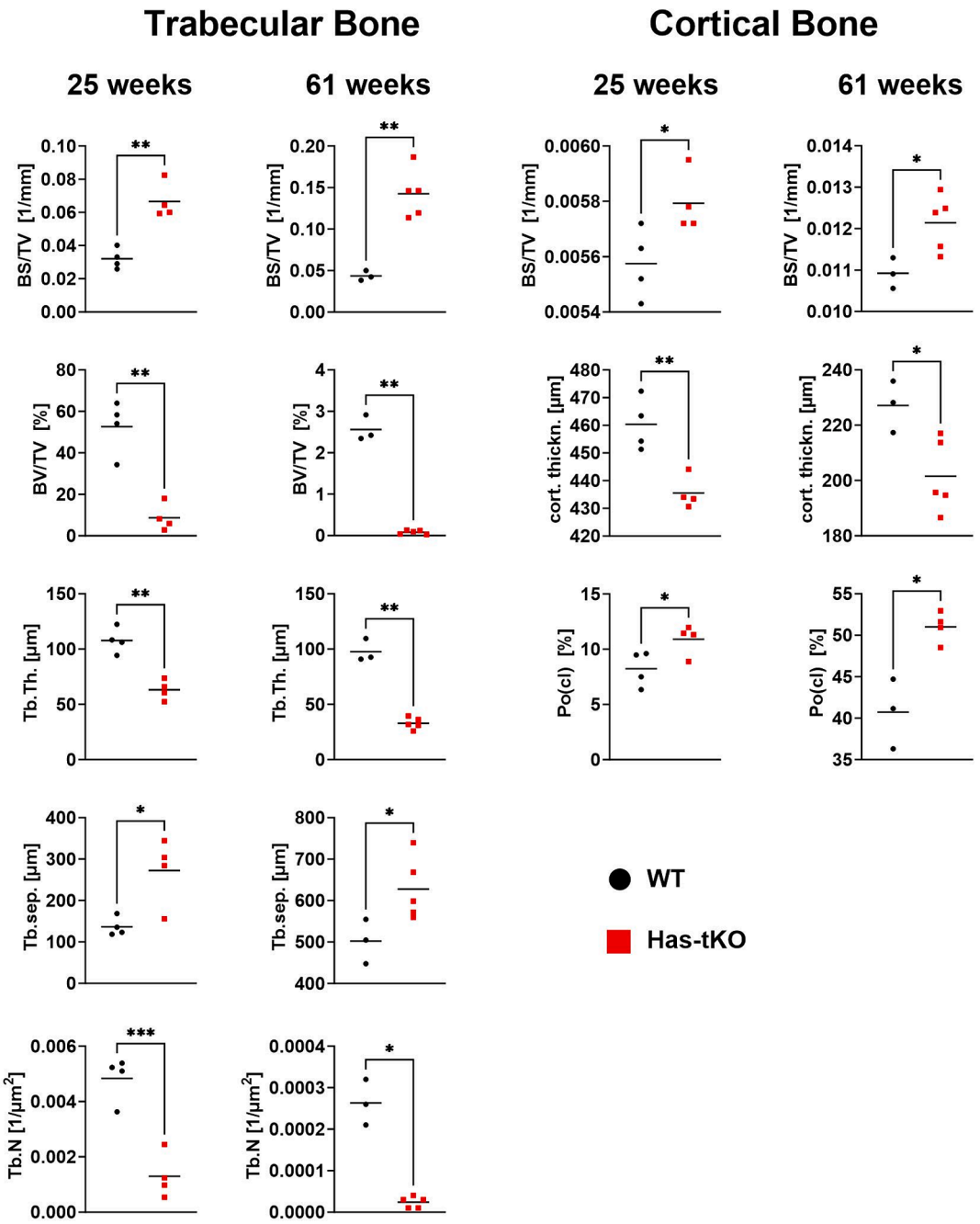

Fig. 4. Loss of HA synthesis leads to reduced bone quality and progresses with age. Two cohorts of age-matched female mice (A-25 weeks and B-61 weeks) treated with tamoxifen between 8 and 10 weeks of age, were used to obtain femurs. C57Bl6 mice were treated equally as wild-type controls. µCT scans were analysed for bone volume/total volume (BV/TV), bone surface/bone volume (BS/BV), trabecular thickness (Tb.Th.), separation (Tb.sep.) and number (Tb.N) in femoral trabecular bone. Bone surface/bone volume (BS/BV), cortial cross-sectional thickness (Cs.Th.) and closed porosity (Po(cl)) were determined in femoral cortical bone. Unpaired *t*-test with Welch's correction, * $p < 0.05$, ** $p < 0.01$, *** $p < 0.0005$.

Table 1).

The observed impaired bone quality does not appear to be due to increased osteoclast activity, as we did not observe differences in TRAP activity in trabecular bone. Bone histomorphometry showed that there were no differences in osteoclast numbers per bone perimeter or osteoclast surface per bone surface between wildtype and Has-tKO derived bones. Furthermore, the expression of osteoclast-related genes such as the essential transcription factor Nfatc1, the differentiation and activation factor RankL, Oscar or the phosphatase Trap (Acp5) did not differ between the genotypes (Supplemental Fig. 4).

Collectively, these data suggest that bone phenotype induced by abrogation of HA synthesis is similar in females and males. The effects are detectable as early as five weeks after introducing the full knockout and progress with age.

Loss of HA synthesis capacity impairs osteogenic differentiation of MSC in vitro

Based on previous findings showing the importance of HA during embryonic bone development, we asked whether a direct effect of Has knockout on osteogenic differentiation could lead to the observed reduction in bone mass and quality. Here, we investigated the

osteogenic differentiation of precursor cells depending on their Has expression and HA synthesis *in vitro*. Bone-derived MSC from untreated wild-type and Has-tKO mice were isolated, cultured and treated with 4-hydroxytamoxifen in order to establish the Has2 knockout in the Has-tKO-derived MSC. MSC from Has-tKO mice released significantly less HA into the culture medium than the wild-type MSC receiving the same treatment (Fig. 5A) confirming the desired knockout.

MSC were differentiated in osteogenic differentiation medium for 12 days and the expression of Has enzymes and osteogenic differentiation markers (Runx-2, Tnalp1, Osterix, Osteocalcin) were analysed at days 3, 7 and 12 of differentiation. In addition, cells were stained with alizarin red at days 7 and 12 of differentiation.

First, we show that the expression of Has2 and Has3 is regulated during osteogenic differentiation of wild-type MSC. Has2 was expressed at high levels that further increased during differentiation, whereas Has3 was detected at much lower expression levels which further decreased during differentiation *in vitro* (Fig. 5A-C). In contrast to in wild-type MSCs, Has2 expression did not increase in Has-tKO-derived MSC (Fig. 5B) and Has3 was also not expressed (Fig. 5C). Has1 was not detected neither in wildtype, nor in Has-tKO cells (data not shown).

Next, the mRNA expression of osteogenic differentiation markers was analysed after 7 and 12 days of differentiation in MSC from both genotypes. The expression levels of Runx-2 and Tnalp1 were significantly lower in MSC derived from Has-tKO mice whereas the expression levels of Osterix and Osteocalcin were decreased by trend (Fig. 5D). The impaired osteogenic differentiation of Has-tKO derived MSC was further supported by significantly reduced alizarin red staining at both 7 and 12 days of differentiation (Fig. 5E). We excluded reduced vitality of the Has-tKO MSC after 12 days of differentiation as a cause for these differences (Fig. 5F). To gain deeper insights into the mechanisms of HA-mediated regulation of osteoblast differentiation, we analyzed the signaling mechanisms upon induction of osteoblast differentiation. As shown in Fig. 5G, HA deletion decreased the phosphorylation level of Smad1/5 in MSC from Has-tKO mice upon initial addition of osteogenic differentiation medium (Fig. 5G), suggesting that abrogation of Has expression results in impaired sensitivity to growth factors such as BMP [21]. Thus, fine-tuned expression of Has2 during osteogenic differentiation may be important for *de novo* differentiation of osteoblasts.

Total Has knockout modifies the transcriptome of differentiating MSC

The differentiation experiments suggested that a fine-tuned expression of Has2 during osteogenic differentiation may be important for de novo differentiation of bone cells. In order to evaluate the global transcriptional alterations of tHas-KO MSC during osteogenic differentiation, RNAseq analysis was conducted of differentiating MSC at day 7.

205 transcripts were upregulated in wild-type MSC compared to the Has-tKO MSC, equivalent to a reduced expression in the differentiating MSC from Has-tKO mice (Fig. 6A). GO analysis revealed that wild-type MSC expressed higher levels of genes associated with organ development (e.g. skeletal system, bone morphogenesis and mineralisation, ossification; Fig. 6B), demonstrating the impaired osteogenic differentiation status of MSC from Has-tKO mice. The most relevant bone development genes upregulated in wild-type MSC are listed in Table 1. Although being excluded by the stringent selection criteria for identifying differentially expressed genes during RNA-seq analysis (2fold differential expression and $p < 0.05$), the osteogenic transcription factors Runx-2 and Sp7 were also higher expressed in wild-type MSC (Table 1).

In addition, 297 genes were significantly upregulated in Has-tKO compared to wild-type control cells. MSC from Has-tKO mice were characterised by inflammatory activation rather than bone development (Fig. 6C). As shown in Table 2, upregulated genes in MSC from Has-tKO mice are mostly related to chemokine activity and cytokine signalling categories and their activities have also have been assigned to bone synthesis and turnover.

To validate the *in vitro* differentiation findings, we investigated whether some of these differences may be detected also in bone tissues. Indeed, for Lif, Osm and Cxcl3 we were able to demonstrate increased expression in tibiae from Has-tKO mice 5 weeks after induction of complete Has knockout (Fig. 6D).

Discussion

This study explored the impact of activity loss of Has and consequently of HA tissue content reduction in adult mice on bone structure, thought to be of strong relevance during bone loss in postmenopausal women and ongoing age.

To achieve complete abrogation of HA synthesis in adult mice, we generated a novel Has-total knockout mouse model in which a constitutive knockout of Has1 and Has3 was combined with an inducible, Ubc-Cre-driven Has2 knockout. This allows complete KO of Has at any time of life without the problem of induction of compensatory mechanism. In the present study, mice at 8–10 weeks of age were used when the major bone development is completed.

We demonstrated the successful reduction of Has expression and HA deposition in the ECM of different organs including bone. Phenotypically, the mice were unaffected in terms of motor behaviour and energy balance. However, the Has-tKO mice developed a strong phenotype of bone loss, strikingly exceeding that of Has1,3-DKO. These differences were detectable five weeks after induced Has2 knockout and maintained at later age. Importantly, *in vitro* studies showed an impaired osteogenic differentiation capacity of Has-tKO-derived MSC. Whole transcriptome analysis suggests that key processes of bone and matrix formation are impaired in the differentiating MSC upon loss of Has enzymes.

All together, these data strongly point to HA synthesis in particular by the Has2 as major player in bone turnover and remodelling. HA is a part of the extracellular matrix of many organs and can also be found in serum and other body fluids. During embryogenesis, Has2-synthesised HA is essential for bone development. Specifically, it is one of the major components of the hypertrophic zone in the growth plate and is important during chondrocyte condensation, endochondral ossification leading to long bone formation [12,14,22]. Has2 has been shown to be important for the maintenance of the cytoskeleton in chondrocytes [23] and thus their functionality. The cytoskeleton may be regulated via HA-binding to the receptor CD44 and intracellular, associated proteins [24].

In contrast to studies using genetic models during embryogenesis, there is a lack of models analysing the effects of HA turnover in adult mice. The presented novel mouse model allows us to compare the effects of either Has1 and Has3 or additional Has2 at any interesting life situation. A great advantage of our model is that Has2 expression is blocked systemically after reaching juvenile adulthood and does not affect embryonic development as found in previous studies [3]. One limitation of our model is that we cannot distinguish between the contribution of different cell types producing HA. With respect to bone, chondrocytes, osteoblasts, osteocytes, osteoclasts, bone marrow cells and endothelial cells could directly or indirectly contribute to the observed changes, since they typically synthesize HA. Moreover, HA is released into the extracellular space regulating surrounding cells, which might contribute to the phenotype. Our models allow to answer the general question of the role of HA in the maintenance of bone remodeling. Future studies have to identify in detail which cells are the main producers and responders to HA with cell-type specific knockouts.

Here, the constitutive knockout of Has1 and Has3 results in a moderate reduction of resting HA content in many organs and bone. The significant strengthening of this effect by the additional Has2-KO suggests a major contribution of Has2-derived HA to the composition of the extracellular matrix in agreement with results from primary cells from skin, lung and kidney [20,25,26]. Our model of complete abrogation of HA synthesis in mice precludes any compensation of the Has1,3 double knockout by increased Has2 expression as reported in skin of Has1,3-DKO mice [17]. As the expression levels of hyaluronidases are not

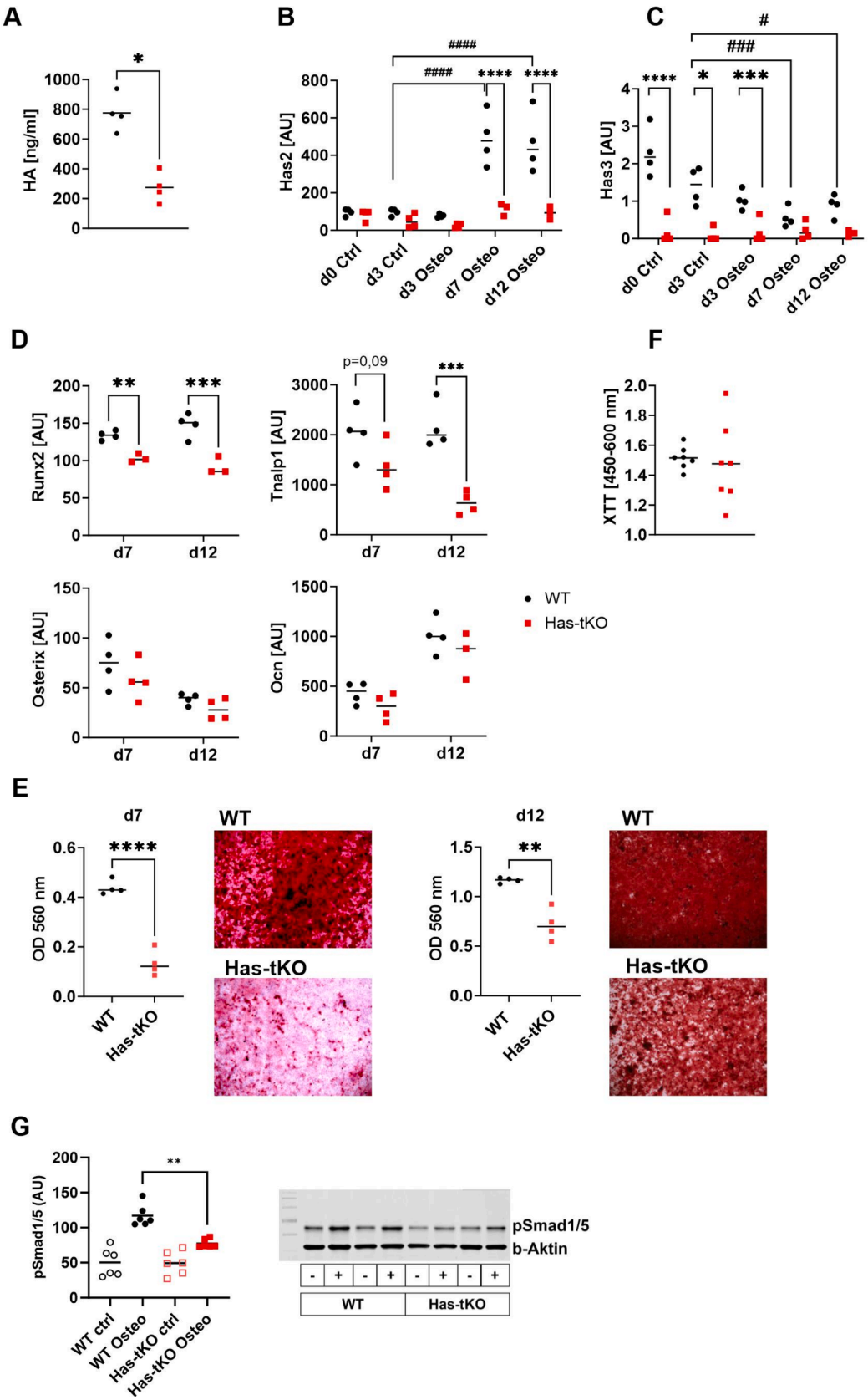

(caption on next page)

Fig. 5. Abrogation of HA synthesis impairs osteogenic MSC differentiation *in vitro*. (A) Regulation of HA synthesis in bone marrow-derived MSC during osteogenic differentiation. Amount of HA released by MSC into the culture supernatant during 48 h before addition of differentiation medium. *p < 0.05 Mann-Whitney test. (B, C) Gene expression of MSC at different time points with control medium or osteogenic differentiation medium. One-way ANOVA *,# p < 0.05; ***,### p < 0.001; ****,#### p < 0.0001. (D) Gene expression levels of Runx2, Tnalp1, Osterix and Osteocalcin (Ocn) were quantified by RT-qPCR at day 7 and day 12 of differentiation. (E) Alizarin red staining of MSC at day 7 and day 12 of differentiation. (F) XTT assay at day 12 of differentiation. 2way ANOVA for gene expression analysis and unpaired Student's T-test for alizarin red OD. **p < 0.01; ***p < 0.001; ****p < 0.0001, (G) Reduced phosphorylation of Smad1/5 in Has-tKO-derived MSC upon addition of osteogenic medium. Densitometry and representative blot. n = 6, One-way ANOVA, **p < 0.01. (For interpretation of the references to colour in this figure legend, the reader is referred to the web version of this article.)

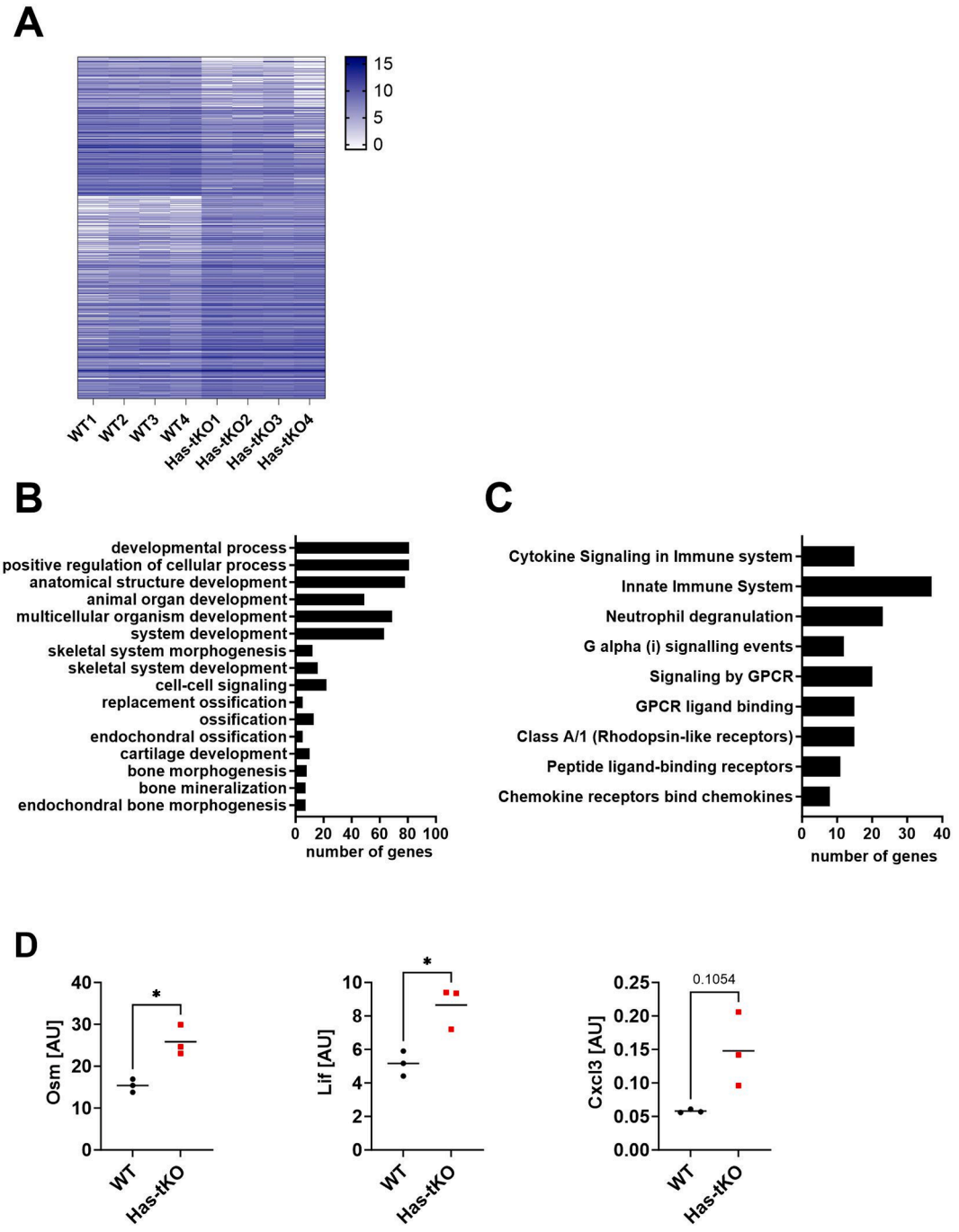

Fig. 6. Has knockout in MSC results in modified transcriptomes during osteogenic differentiation. Different gene expression patterns in wild-type and Has-tKO derived MSC during osteogenic differentiation (A). MSC from wild-type mice are characterised by increased expression of genes related to bone morphogenesis (B), when Has-tKO-derived MSC show increased expression of inflammation-related genes, especially chemokines (C). Differential expression of Oncostatin m, Cxcl3 and Lif was detected *in vivo* in tibiae of WT and Has-tKO mice. *p < 0.05, Student's T-test with Welch's correction (D).

Table 1
Ossification-related genes, significantly upregulated in MSC from WT mice at day7 during osteogenic differentiation *in vitro*.

GENE	DESCRIPTION	Nfold WT/Has-tKO	p Value
Alpl	Alkaline phosphatase, tissue-nonspecific isozyme	2.52	0.014
Cbs	Cystathionine beta-synthase	5.08	0.015
Clec3a	C-type lectin domain family 3 member A	5.06	0.032
Col10a1	Collagen alpha-1(X) chain	2.73	0.010
Cthrc1	Collagen triple helix repeat-containing protein 1	2.13	0.030
Fgfr3	Fibroblast growth factor receptor 3	2.21	0.001
Fzd9	Frizzled-9	2.49	0.031
Ibsp	Bone sialoprotein 2	2.31	0.009
Lrrc17	Leucine-rich repeat-containing protein 17	2.01	0.002
Phospho1	Phosphoethanolamine_phosphocholine phosphatase	3.29	0.014
Pth1r	Parathyroid hormone_parathyroid hormone-related peptide receptor	2.46	0.017
Smpd3	Sphingomyelin phosphodiesterase 3	4.01	0.033
Sox9	Transcription factor SOX-9	2.13	0.002
Runx-2	*Osteogenic transcription factor*	*1.52*	*0.023*
Sp7	*Osterix (bone specific transcription factor)*	*1.89*	*0.083*

Table 2
Genes, significantly upregulated in MSC from Has-tKo mice at day7 of osteogenic differentiation *in vitro* representing chemokine related interactions and cytokine signalling.

PROCESS	GENE	DESCRIPTION	Nfold Has-tKO/WT	p Value
Chemokine receptors bind chemokines	Ccl20	C-C motif chemokine 20	71.35	0.033
	Ccl3	C-C motif chemokine 3	8.86	0.023
	Ccl4	C-C motif chemokine 4	8.03	0.005
	Ccr2	C-C chemokine receptor type 2	8.89	0.021
	Ccr5	C-C chemokine receptor type 5	3.67	0.005
	Ccrl2	C-C chemokine receptor-like 2	5.51	0.048
	Cx3cl1	Fractalkine	2.11	0.007
	Cxcl2	C-X-C motif chemokine 2	6.53	0.002
	Cxcr4	C-X-C chemokine receptor type 4	2.15	0.002
Cytokine Signaling in Immune system	Clcf1	Cardiotrophin-like cytokine factor 1	2.28	0.028
	Dusp6	Dual specificity protein phosphatase 6	2.73	0.0006
	Ebi3	Interleukin-27 subunit beta	2.38	0.016
	Hck	Tyrosine-protein kinase HCK	3.50	0.026
	Il21r	Interleukin-21 receptor	3.75	0.022
	Lif	Leukemia inhibitory factor	5.16	0.004
	Nfkb2	Nuclear factor NF-kappa-B p100 subunit	2.53	0.015
	Osm	Oncostatin-M	4.07	0.031
	Ptpn6	Tyrosine-protein phosphatase non-receptor type 6	2.1	0.003
	Relb	Transcription factor RelB	2.02	0.0003
	Ripk2	Receptor-interacting serine_threonine-protein kinase 2	2.18	0.046
	Sla	Src-like-adapter	2.03	0.039
	Socs3	Suppressor of cytokine signaling 3	2.15	0.003
	Tnf	Tumor necrosis factor	3.46	0.011
	Tnfrsf12a	Tumor necrosis factor receptor superfamily member 12A	2.19	0.008

affected, the reduced HA concentrations in the mouse tissues are due to the inhibition of HA synthesis.

Despite the strong modulation of HA content in the matrix of many organs the knockout does not affect the overall phenotype of the mice. They grow and breed normally and do not differ in their voluntary activity, suggesting that they do not experience disabilities such as osteoarthritis or joint pain that limit their activity. However, we cannot exclude that the duration of the additional Has2-KO was too short to evoke measurable impairments. Furthermore, the similarity in heat production and respiratory exchange rates does not suggest that the systemic elimination of HA synthesis, which is a highly energy-consuming process [20], results in a significant phenotype. Apparently, the organism is able to compensate for the systemic loss of this major matrix component and putative compensatory mechanisms are of interest for further research and may indicate ways to counteract the loss of Has in therapies with glucocorticoids [27,28].

An earlier study on Has1$^{-/-}$, Has3$^{-/-}$ or Has1,3-DKO mice reported differences in the retrocalcaneal bursa but did not report severe physical or developmental defects of their bones and cartilage [29]. Similarly, in our cohorts, the constitutive Has1,3 knockout mildly affects trabecular and cortical bone quality. The changes were mild and limited to trabecular bone, with a decrease in bone volume and number of trabeculae in the femurs. Pendyala et al. described that constitutive knockout of Has1 reduced bone cross-sectional area and reduced mineral to matrix ratio, whereas Has3 knockout resulted in increased mineral to matrix ratio and higher stiffness in adult mice [16].

In young adult Has-tKO mice, the reduced bone HA content was accompanied by diminished bending stiffness in accordance with the physiological function of HA e.g., stabilizing extracellular matrix structure by binding to proteoglycans [8]. However, the cortical bone density was not related to Has depletion as Calcium hydroxyapatite content did not differ between the mouse strains.

As bone quality is known to decline with age and postmenopausal women are frequently affected by these problems [28], we analysed the femurs of older female mice (25 weeks and 61 weeks) by μCT. The ageing phenomena of reduced bone quality were detected in both wild-type and HAS-tKO mice. In addition, complete abolition of HA synthesis resulted in trabecular bone characteristics in younger Has-tKO mice that were similar to those in aged wild-type mice (61 weeks), but progressed even further with age. Cortical bone was thinner in Has-tKO, which was further enhanced in the aged cohort. These data indicate that (i) there is active HA turnover in adult bone and (ii) HA synthesis and renewal are also important in adult mice, and that abrogation of HA synthesis results in bone phenotypes resembling aged bone.

These HA-related findings are in agreement with promoting osteoblast differentiation [30–32] and counteracting IL-1β-driven osteoclastic bone resorption [33] by high molecular weight HA *in vitro*. HA-based biomaterials have been shown to support the healing of critical bone defects [34–36], suggesting that endogenous HA is critical for bone regeneration.

Our data strongly suggest alterations in the osteogenic differentiation of MSC. Indeed, Has2 is upregulated in differentiating wild-type MSC, which consistent with impaired embryonic bone development in conditionally Has2-depleted mice and cells [12–14]. Thus, MSC from Has-tKO mice show a disturbed osteogenic differentiation indicated by a reduced activation of the Smad1/5 signalling pathway followed by diminished expression of osteogenic markers compared to wild-type MSC detailed in Fig. 5. Currently, it remains an open question how the lack of HA contributes to these effects. HA loss can result in a modified clustering of the HA receptor Cd44 putatively leading to disturbed receptor signalling platforms [37,38]. However, Cd44 expression is not modified in MSC of Has-tKO mice.

Although the *in vitro* differentiation model is rather simple and lacks 3D structure and niche components, the RNAseq data at day 7 of differentiation (Tab.1) show a decreased expression of genes critically involved in bone growth such as Sox9 [39], Fzd9 [40], Ibsp [41], Fgfr3

[42], Smpd3 [43] These differences compared to wild-type MSC very likely cause the disturbed bone architecture in Has-tKO mice observed by μCT.

On the other hand, the Has-tKO induces a strong phenotype of chemokine secretion and cytokine signalling. in differentiating MSC [44]. The significantly induced leucemia inhibitory factor (Lif) represses osteoblast differentiation in fetal rat calvarial system related to Has2 expression [15]. Thus, the induction of Lif in the differentiating MSC from the Has-tKO mice is consistent with the observed phenotype of trabecular and cortical bone. Many of the induced chemokines and cytokines in Has-tKO-derived MSC shown in Table 2 are related to bone loss (IL-21 [44]) or impaired bone growth (Relb and NfkB2 [45]). These *in vitro* findings could be verified *in vivo* by gene expression analysis in tibiae of Has-tKO mice. The increased expression of Clcf1 by MSC from Has-tKO could have paracrine effects on osteoclast progenitors, repressing there the nuclear factor-κB pathway and osteoclast activity [46], which may contribute to the unchanged osteoclast phenotype observed by bone histomorphometry and gene expression of osteoclast markers in these mice.

Bone turnover depends on a regulated balance between osteoclast and osteoblast activity, with osteoclast activity also being important for the subsequent bone remodelling by osteoblasts. The role of HA in this interplay is not clear, with conflicting data in the literature, possibly due to the *in vivo* model or *in vitro* culture conditions used. Broadly speaking, high-molecular-weight-HA is considered to be pro-osteogenic and inhibits osteoclastogenesis as has been found in a model with systemic application of HA to ovariectomiced rats [47].

In the same line of evidence, *in vitro* findings show that glucosamine supports Has-expression, HA synthesis and osteoblastic cell differentiation, but decreases the expression of receptor activator of NF-κB ligand (RANKL), which would induce osteoclastogenesis [48]. The inhibition of RANKL through the Rho kinase pathway is a mechanism involving CD44-HA interaction [49].

This interaction of HMW-HA with its receptor Cd44 is putatively involved in the balance of osteoblast and osteoclast activity. Thus, Cd44 is important for osteoclast differentiation *in vitro,* as shown in studies using bone marrow-derived osteoclasts from wildtype and $Cd44^{-/-}$ mice. Here, Cd44-knockout impaired NfKB signalling and the subsequent formation of RANK-Traf6 complexes [50]. On the other hand, differentiated osteoclasts bind HA *in vitro* via Cd44, leading to downregulation of proteases, increased phosphorylation of Pyk2 and p38, and consequent downregulation of the critical transcription factor Nfatc1 [51]. Interestingly, the effect of Cd44 seems to be strongly dependent on the experimental conditions, as no differences in the number of multinucleated cells or in bone resorption were observed when osteoclasts were generated *in vitro* on bone tissue instead of on plastic. [52].

Many effects of HA depend on their molecular size. Chang et al. [53] investigated the effect of exogenous HA of different sizes on osteoclastogenesis *in vitro*. In their model, HMW-HA suppressed osteoclastogenesis depending on Toll-like receptor 4 (TLR4). HA sized below 230 kDa induced the osteoclast TRAP activity. Moreover, antibody-mediated Cd44 blocking did not affect the HA effects supporting the findings by de Vries et al. [52]. In an *in vivo* mouse model of calvarial bone resorption HMW-HA could decrease RANKL-induced bone erosion and osteoclastogenesis [53]. As above, Low Molecular Weight-HA has been shown to enhance osteoclast formation and function [54]. It acts mainly through TLR4 which was found to be essential for osteoclastogenesis [55]. However, LMW-HA also could inhibit osteoclast differentiation of RAW264.7 cells reducing their TRAP activity and expression of osteoclast marker genes *in vitro* [56]. In our Has-tKO mice, presumably also the amount of LMW-HA is decreased what might influence the rate of TLR4 signalling, especially in unchallenged mice. Similar to our findings, a conditional Has2-KO in chondrocytes resulted in a severe bone phenotype, but did not modify the detected number of osteoclasts in mouse embryonal bones at E18.5 [12]. We could not find differences in expression levels of osteoclast markers like Nfatc1, Trap (Acp5), or Oscar in bone of Has-tKO mice and in TRAP staining of femurs (Suppl. Fig. 4), suggesting that the observed bone loss does not result from increased bone resorption but more likely from compromised osteogenesis. However, further investigations are required to decipher the role of osteoclast activation and bone resorption in this regard.

Taken together, we have developed a unique set of mouse strains that allow us to dissect the impact of individual HA synthases on tissue architecture, stability and function in adult mice. In addition, pathophysiological processes such as inflammation, tissue repair or ageing can be studied with respect to the role of individual HA-synthases at the whole organism level, but also at the level of key cell types involved.

In mouse bone, our data indicate that Has2 and Has3 are the predominant HA synthases and that sufficient HA synthesis is essential for maintaining bone quality *in vivo*. Mechanistically, abrogated HA synthesis affects the osteogenic differentiation of stem cells, leading at least in part to the observed phenotype. Future research utilizing our mouse models may provide answers to the physiological and pathological decline of HA levels as a contributor to age-related bone disease.

Materials and Methods

Mice

The generation of the $Has2^{fl/fl}$ mice was first described in [57]. A modified Cre recombinase, linked to a mutated estrogen receptor (Cre^{ERT2}) under the control of the ubiquitously expressed ubiquitin C promotor (UbC) was used to generate an inducible knockout of Has2 (Has2-cKO) [57]. The Has1,3-DKO mice were generously provided by the lab of E. Maytin (Cleveland Clinic, Cleveland OH) and have constitutive $Has1^{-/-}$, $Has3^{-/-}$ allele distribution in the whole body. These mice do not exhibit any apparent developmental abnormalities and have normal life span [17] and breeding efficiency.

Has2cKO as well as Has1,3 DKO mice were used to create the Has-tKO mice, by crossing $Cre^{+/-}$ Has2-cKO mice with Has1,3-DKO mice. Heterozygous F1 generations were mated to finally obtain $Has1^{-/-}$; $Has3^{-/-}$; UbC-$Cre^{ERT2+/-}$ $Has2^{fl/fl}$ animals. In the following, the C57/BL6-Has1,3KO- UbC-$Cre^{ERT2+/-}$-$HAS2^{fl/fl}$ lineage was used as Has-tKO and Cre negative animals (UbC-$Cre^{ERT2-/-}$) represent the Has1,3 DKO mice. The wildtype controls were of the parental C57Bl6J strain and treated in parallel.

All animal experiments were performed following institutional and state guidelines and approved by the Committee on Animal Welfare of Saxony (TVV 54/20, TVV 26/19, T05/20). Mice were kept under a 12-hour light–dark cycle and given food and water ad libitum. The mice were under routine surveillance for pathogens. Mice at age of 8–10 weeks were injected i.p. with tamoxifen (25 mg/ml in sunflower seed oil (Sigma T5648 and S5007 respectively, 100 μl per injection for 5 days) followed by a resting phase of minimal 5 weeks to establish the Has2-knockout.

Phenotypic investigation

The PhenoMaster® (TSE-Systems, Berlin Germany) was used to monitor mice of all strains, in parallel with a high resolution for voluntary wheel activity, calorimetry and standard chow consumption (SC) (EF V1534-000, Sniff Spezialdiäten GmbH). Oxygen consumption and carbon dioxide production were measured through an open-circuit indirect calorimetry system in eight individual cages used to calculate the respiratory exchange ratio (RER). Oxygen and carbondioxide sensors were calibrated with calibration gas mixtures of CO2 and O2 in N2 (Air liquid Deutschland GmbH, Germany) and the sample airflow. Mice (25 weeks old) were adapted for 12 h in the light phase in the metabolic cages and monitored for 3 dark and 3 light phases. Mice (61 weeks old) were monitored for two light and dark phases, each. The data of dark and light phases were combined.

Assessment of bone by MicroCT (μCT]

Femurs were fixed for 48 h in 4 % paraformaldehyde (Carl Roth, P087.5) and then dehydrated in 80 % ethanol. MicroCT measurements were carried out on femur bones with the SkyScan1176 μCT (Bruker, Billerica, MA, USA) using a 50 μm aluminum filter at 50 kV, 500μA, 9 μm voxel size and a 1° rotation step. The analysis of trabecular and cortical bone volume per total volume (BV/TV), thickness (Tb.Th and Ct.Th for the trabecular and cortical thickness, respectively), and cortical porosity (Ct.Po) was performed using established analysis protocols and the μCT parameters were reported according to international guidelines [58]. For tissue mineral density measurements the bones were rehydrated in PBS and phantoms of 0.25 g and 0.75 g CaHA/cm3 (Bruker) were scanned the same day for calibration.

Biomechanical testing: Reference-point analysis and three-point bending test

Femurs were shock-frozen in liquid nitrogen and stored at − 80 °C. The bones were thawed 5 min before reference-point indentation (BioDent2, ActiveLife Scientific). Bones were stabilized using an ex vivo small bone stage filled with PBS to avoid sample drying. The reference probe was located at the anterior side of the femur shaft, and indentation measurements were performed (2 N, five cycles) in triplicate for each bone sample by lifting up of the measurement head unit and movement of the sample by a minimum. The first cycle indentation distance (CID 1st) and total distance increase (TID) were calculated. Immediately afterward, the bone samples were mechanically tested in a non-destructive three-point bending test (Zwick material testing machine). Load was applied at the anterior site of the femoral shaft, and the bending stiffness was calculated using the slope of the load–deflection curve.

Purification, culture and osteogenic differentiation of BM-derived MSC

MSC were purified from femora and tibiae of the hind legs of wild-type and Has-tKO mice as described previously [59]. The cells were cultured for 4 passages in a-MEM (Lonza, 12–169) supplemented with stabilized glutamine (ThermoFisherScientific, 25030081) and 10 % FCS (anprotec, AC-SM-0190). Addition of 4-hydroxytamoxifen (2 mM, Hycultec, HY-16950) for 48 h during passages 2 and 3 introduced the inducible knockout of Has2 in the cells which was verified by HA-ELISA of the supernatants and Has2-qRT PCR. Osteogenic differentiation was induced with the StemXVivo Osteogenic medium and supplement (Biotechne, CCM007/9) for 12 days with medium exchange every 3 days.

Calcification was verified by Alizarin red staining. Cells were washed with PBS, fixed in 10 % paraformaldehyde for 15 min at RT, washed with a.d., and stained with Alizarin red solution (Sigma, TMS-008-C). After several washes with water, the cells were photographed with a BZ-800x microscope (Keyence). Later, the dye was solubilized by 100 mM hexadecylpyridinium chloride monohydrate (Sigma, 840008) for 30 min, and absorption at 540 nm was measured at a BioTek Synergy HT microplate reader (BioTek Instruments) [59].

Phosphorylation analysis

Undifferentiated, hydroxytamoxifen treated MSC were plated into 12 wells ($1.5x10^6$ per well). After 24 h of culture in complete aMEM, the medium was replaced with StemXVivo Osteogenic Medium and Supplement for 30 min. Cells were lysed with SDS cell lysis buffer (Cell Signaling Technologies) and subjected to Western blotting on PVDF membrane (Merck-Millipore). Phosphorylated Smad 1/5 (Cell signalling technologies, #9516) was detected with goat anti-rabbit-800 secondary antibody (LICORbio #926–32211); equal loading was verified with Revert™ 520 total protein stain (LICORbio #926–10011) and b-actin reference gene (LICORbio #926–42212) was detected with goat anti-mouse680RD (LICORbio #926–6807) on a LICORbio DLX scanner. For quantification, the pSmad 1/5 signal was divided by the b-Actin signal.

RNA isolation and gene expression analysis

RNA was isolated using the column extraction kit ReliaPrep™ RNA Miniprep System (Promega, Z6112). Bones were minced in lysis buffer and the purification procedure was finished according to manufacturer's protocol. The same kit was used to purify RNA from cultured MSC. The concentration and purity of the RNA solution was measured by spectrophotometer (BIOTEK Synergy HT equipped with a special nanoplate).

300 ng RNA was subjected to reverse transcription to complementary DNA (cDNA) with the LunaScript® RT SuperMix Kit (NEB, E3010L). For gene expression analysis, cDNA was diluted by the addition of 80 μL nuclease-free water (1:5 dilution) before storage at −80 °C.

The qPCR of the cDNA was performed using Luna® Universal qPCR Master Mix (NEB, M3003E). Plasmids (pJet1.2, ThermoFisherSci) containing cloned cDNA of the respective GOI were used for absolute quantitation from a standard curve. The reference gene Rplp0 was used as control and a melt curve was generated to control amplification specificity. Primer sequences are given in Suppl.Tab.2.

RNA sequencing analysis of cultured MSC under osteogenic differentiation

RNA from MSC at day 7 of osteogenic differentiation (n = 4 per group) was purified with the Reliaprep RNA purification system (Promega). RNA integrity and concentration were examined on an Agilent Fragment Analyzer (Agilent Technologies, Palo Alto, CA, USA) using the HS RNA Kit (Agilent 5067–1513) according to the manufacturer's instructions.

RNA sequencing was performed at the Core unit DNA technologies of the Leipzig University (Dr. K. Krohn). Briefly,100 ng of total RNA was depleted of ribosomal RNA using the NEBNext® rRNA Depletion Kit v2 (NEB) according to the instructions of the manufacturer. Depleted RNA was transcribed using SuperScript IV reverse transcriptase (ThermoFisher, 18090200) for 2 h at 55 °C. After second strand synthesis (TargetAmp kit, Epicentre), DNA was treated with the Illumina Tagment DNA TDE1 Enzyme and Buffer Kits, which fragments the DNA and inserts partial sequencing adapter (Nextera) sequences. Final PCR amplification of the libraries was done using KAPA HiFi HotStart Library Amplification Kit with unique dual indexing by IDT® for Illumina Nextera DNA Unique Dual Indexes Sets. The purified barcoded libraries were quantified using Qubit Fluorometric Quantification (ThermoFischer Scientific). The size distribution of the library DNA was analyzed using the FragmentAnalyzer (Agilent). Sequencing of 2x150 bp was performed with a NovaSeq6000 sequencer (Illumina) according to manufacturer's instructions. After demultiplexing with *bcl2fastq* software (Illumina, v2.20) and polishing using *fastp* [60] only sequences longer than 20 bp were further analyzed. Reads were mapped against the mouse reference genome (GRCm39) using HISAT2 [61]. Stringtie and the R package Ballgown [62] were employed to calculate differential expression. Expression data were normalized using the DESeq2 R bioconductor package [63]. For data analysis, a total of 53,600 genes were counted. The mean of signal strength of wild-type and Has-tKO, p-value (Student's *t*-test) and x-fold change were calculated. Genes between 0.5 and 2-fold change and a p-value < 0.05 were put into GO-biological process and reactome pathway analyses [64,65]. Resulting hits were log2-transformed and plotted in the heatmap using Graphpad Prism10.0.2.

HA-quantification (HA-ELISA)

For direct quantification of HA, tissue samples were taken, shortly dried on filter paper and weighted (wet-weight). For tissue lysis, samples were incubated with 20 U/mL Protease from Streptomyces griseus

(Sigma, P5147) and 5 mM deferoxamine mesylate salt (Sigma, D9533) dissolved in HA-prep buffer (150 mM Tris, 150 mM NaCl, 10 mM CaCl2, pH = 8.3). Bones were mechanically disrupted with steel beads in digestion buffer. After shaking overnight at 55 °C, the protease was inactivated by heating at 95 °C for 10 min. Afterwards, the lysate was centrifuged at 20,000 × g at 4 °C for 15 min. Alternatively, cell culture supernatant from equal cell numbers seeded was collected after 48 h and analysed. Finally, HA- concentration was quantified using a commercial HA-ELISA Kit (TECOmedical, TE1017-2) according to the original protocol.

TRAP staining

Femurs were fixed in 4 % paraformaldehyde for 48 h, decalcified in EDTA (20 %) for two weeks, dehydrated and embedded in paraffin. Paraffin sections were rehydrated and stained using the TRAP staining kit according to the manufacturer's protocol (CosmoBio, Japan, AK04F). Specimens were counterstained with Haemalaun und coverslipped with Aquatex (Merck). Specimens were visualised using a Keyence BX-800 microscope and firmware (Keyence, Germany).

Viability testing (XTTII)

Cell proliferation/vitality was measured with a cell proliferation kit II (XTT) (Roche). 2 thousand cells were seeded in a 96-well cell culture plate. Cells were cultivated in aMEM (10 % FCS, 1 % P/S, glutamine) at 37 °C, 5 % CO2 and 95 % humidity for 24 h. Next day the medium was replaced with aMEM (0.5 % FCS, 1 % P/S, Glutamine) for 24 h in order to synchronize the cells. After synchronization, the medium was replaced back to normal growth medium for 48 h. Medium was replaced with medium containing XTT reagent (0,3mg/ml final conc.) and the absorbance (OD 452/650 nm) was measured immediately after addition and 2 h of incubation.

Statistical analysis

Statistical analysis for two-group comparisons regarding normally distributed metrical data was performed using two-tailed Student's *t* test. Normality was tested by D'Agostino & Pearson's Normality test or Shapiro-Wilk-Test ($n \leq 4$). Where normality was absent, Mann-Whitney test was used. For statistical comparison of more than two groups, ANOVA Test was used. Calculations were done using GraphPad Prism version 10. p-values of 0.05 or smaller were considered statistically significant. The different degrees of significance were indicated as followed: * $p < 0.05$; ** $p < 0.01$; *** $p < 0.005$, **** $p < 0.0001$.

Declaration of Generative AI and AI-assisted technologies in the writing process'

During the preparation of this work the authors did not use Generative AI and AI-assisted technologies. DeepLWrite (https://www.deepl.com/de/write) was used to check and improve English grammar and style. After using this tool/service, the author(s) reviewed and edited the content as needed and take(s) full responsibility for the content of the publication.

CRediT authorship contribution statement

A. Saalbach: Writing – review & editing, Supervision, Methodology, Investigation, Formal analysis, Data curation, Conceptualization. **M. Stein:** Writing – review & editing, Writing – original draft, Visualization, Validation, Methodology, Investigation, Formal analysis, Data curation. **S. Lee:** Writing – review & editing, Methodology, Data curation. **U. Krügel:** Writing – review & editing, Methodology, Investigation, Formal analysis, Data curation. **M. Haffner-Luntzer:** Writing – review & editing, Methodology, Investigation, Data curation. **K. Krohn:** Writing – review & editing, Methodology, Investigation, Formal analysis, Data curation. **S. Franz:** Writing – review & editing, Methodology. **J.C. Simon:** Writing – review & editing, Resources, Funding acquisition, Conceptualization. **J. Tuckermann:** Writing – review & editing, Methodology. **U. Anderegg:** Writing – review & editing, Writing – original draft, Visualization, Validation, Supervision, Project administration, Methodology, Investigation, Funding acquisition, Formal analysis, Conceptualization.

Declaration of competing interest

The authors declare that they have no known competing financial interests or personal relationships that could have appeared to influence the work reported in this paper.

Acknowledgements

Work was supported by Deutsche Forschungsgemeinschaft (DFG) (TRR67 (Project number 59307082)-TPB4 and AN276/6-1 to UA), the Medical Faculty of the University of Leipzig to AS, JCS and UA and by DFG (CRC/SFB 1149 – (Project number 251293561)) to JT.

We greatly appreciate the excellent technical assistance of Mrs. Annett Majok, Mr. Danny Gutknecht and the support by the team of Dr. Knut Krohn who performed and validated the RNA-seq experiments. Dr. Tom Wippold substantially contributed with mouse breeding and strain characterization. We thank Prof. Ed Maytin (Cleveland Clinic, OH, USA) for providing us with Has1,3-KO mice.

Appendix A. Supplementary data

Supplementary data to this article can be found online at https://doi.org/10.1016/j.mbplus.2024.100163.

References

[1] R. Florencio-Silva G.R. da S. Sasso, E. Sasso-Cerri, M.J. Simões, P.S. Cerri, Biology of Bone Tissue: Structure, Function, and Factors That Influence Bone Cells., Biomed Res Int 2015 2015 10.1155/2015/421746 421746.
[2] K.J. Noonan, J.W. Stevens, R. Tammi, M. Tammi, J.A. Hernandez, R.J. Midura, Spatial distribution of CD44 and hyaluronan in the proximal tibia of the growing rat, J. Orthop. Res. 14 (1996) 573–581, https://doi.org/10.1002/jor.1100140411.
[3] T.D. Camenisch, A.P. Spicer, T. Brehm-Gibson, J. Biesterfeldt, M.L. Augustine, A. Calabro, S. Kubalak, S.E. Klewer, J.A. McDonald, Disruption of hyaluronan synthase-2 abrogates normal cardiac morphogenesis and hyaluronan-mediated transformation of epithelium to mesenchyme, J Clin Invest 106 (2000) 349–360, https://doi.org/10.1172/JCI10272.
[4] A.P. Spicer, J.A. Mcdonald, Characterization and Molecular Evolution of a Vertebrate Hyaluronan, Synthase Gene Family* (1998), https://doi.org/10.1074/jbc.273.4.1923.
[5] E.R. Bastow, S. Byers, S.B. Golub, C.E. Clarkin, A.A. Pitsillides, A.J. Fosang, Hyaluronan synthesis and degradation in cartilage and bone, Cell. Mol. Life Sci. 65 (2008) 395–413, https://doi.org/10.1007/s00018-007-7360-z.
[6] R. Tammi, U.M. Agren, A.L. Tuhkanen, M. Tammi, Hyaluronan metabolism in skin, Prog. Histochem. Cytochem. 29 (1994) 1–81.
[7] P.H. Weigel, V.C. Hascall, M. Tammi, Hyaluronan synthases, J Biol Chem 272 (1997) 13997–14000, https://doi.org/10.1074/JBC.272.22.13997.
[8] B.P. Toole, Hyaluronan: from extracellular glue to pericellular cue, Nat Rev Cancer 4 (2004) 528–539, https://doi.org/10.1038/nrc1391.
[9] U. Anderegg, J.C. Simon, M. Averbeck, More than just a filler - the role of hyaluronan for skin homeostasis, Exp. Dermatol. 23 (2014) 295–303.
[10] A.J. Day, C.M. Milner, TSG-6: A multifunctional protein with anti-inflammatory and tissue-protective properties, Matrix Biol. 78–79 (2019) 60–83, https://doi.org/10.1016/j.matbio.2018.01.011.
[11] A.D. Recklies, C. White, L. Melching, P.J. Roughley, Differential regulation and expression of hyaluronan synthases in human articular chondrocytes, synovial cells and osteosarcoma cells, Biochem J 354 (2001) 17–24, https://doi.org/10.1042/0264-6021:3540017.
[12] P. Moffatt, E.R. Lee, B. St-Jacques, K. Matsumoto, Y. Yamaguchi, P.J. Roughley, Hyaluronan production by means of Has2 gene expression in chondrocytes is essential for long bone development, Dev Dyn 240 (2011) 404–412, https://doi.org/10.1002/dvdy.22529.
[13] Y. Li, B.P. Toole, C.N. Dealy, R.A. Kosher, Hyaluronan in limb morphogenesis, Dev Biol 305 (2007) 411–420, https://doi.org/10.1016/j.ydbio.2007.02.023.
[14] K. Matsumoto, Y. Li, C. Jakuba, Y. Sugiyama, T. Sayo, M. Okuno, C.N. Dealy, B. P. Toole, J. Takeda, Y. Yamaguchi, R.A. Kosher, Conditional inactivation of Has2

reveals a crucial role for hyaluronan in skeletal growth, patterning, chondrocyte maturation and joint formation in the developing limb, Development 136 (2009) 2825–2835, https://doi.org/10.1242/dev.038505.
[15] D. Falconi, J. Aubin, LIF inhibits osteoblast differentiation at least in part by regulation of HAS2 and its product hyaluronan, J Bone Miner Res 22 (2007) 1289–1300, https://doi.org/10.1359/JBMR.070417.
[16] M. Pendyala, S.J. Stephen, D. Vashishth, E.A. Blaber, D.D. Chan, Loss of hyaluronan synthases impacts bone morphology, quality, and mechanical properties, Bone 172 (2023) 116779, https://doi.org/10.1016/j.bone.2023.116779.
[17] J.A. Mack, R.J. Feldman, N. Itano, K. Kimata, M. Lauer, V.C. Hascall, E.V. Maytin, Enhanced inflammation and accelerated wound closure following tetraphorbol ester application or full-thickness wounding in mice lacking hyaluronan synthases Has1 and Has3, J Invest Dermatol 132 (2012) 198–207, https://doi.org/10.1038/jid.2011.248.
[18] N.S. Fedarko, U.K. Vetter, S. Weinstein, P.G. Robey, Age-related changes in hyaluronan, proteoglycan, collagen, and osteonectin synthesis by human bone cells, J Cell Physiol 151 (1992) 215–227, https://doi.org/10.1002/jcp.1041510202.
[19] D. Vigetti, M. Viola, E. Karousou, G. De Luca, A. Passi, Metabolic control of hyaluronan synthases, Matrix Biol. 35 (2014) 8–13, https://doi.org/10.1016/J.MATBIO.2013.10.002.
[20] I. Caon, A. Parnigoni, M. Viola, E. Karousou, A. Passi, D. Vigetti, Cell Energy Metabolism and Hyaluronan Synthesis, J. Histochem. Cytochem. 69 (2021) 35–47, https://doi.org/10.1369/0022155420929772.
[21] M. Kretzschmar, F. Liu, A. Hata, J. Doody, J. Massagué, The TGF-beta family mediator Smad1 is phosphorylated directly and activated functionally by the BMP receptor kinase, Genes Dev 11 (1997) 984–995, https://doi.org/10.1101/gad.11.8.984.
[22] P.J. Roughley, L. Lamplugh, E.R. Lee, K. Matsumoto, Y. Yamaguchi, The role of hyaluronan produced by Has2 gene expression in development of the spine, Spine (Phila Pa 1976) 36 (2011). https://doi.org/10.1097/BRS.0b013e3181f1e84f.
[23] J. Yang, L. Wang, Z. Zhang, Q. Sun, Y. Zhang, Downregulation of HAS-2 regulates the chondrocyte cytoskeleton and induces cartilage degeneration by activating the RhoA/ROCK signaling pathway, Int J Mol Med 52 (2023) 1–14, https://doi.org/10.3892/ijmm.2023.5260.
[24] R.F. Thorne, J.W. Legg, C.M. Isacke, The role of the CD44 transmembrane and cytoplasmic domains in co-ordinating adhesive and signalling events, J Cell Sci 117 (2004) 373–380, https://doi.org/10.1242/jcs.00954.
[25] M. Averbeck, C. Gebhardt, U. Anderegg, J.C. Simon, Suppression of hyaluronan synthase 2 expression reflects the atrophogenic potential of glucocorticoids, Exp Dermatol 19 (2010) 757–759, https://doi.org/10.1111/j.1600-0625.2010.01099.x.
[26] D.R. Michael, A.O. Phillips, A. Krupa, J. Martin, J.E. Redman, A. Altaher, R. D. Neville, J. Webber, M. Kim, T. Bowen, The human hyaluronan synthase 2 (HAS2) gene and its natural antisense RNA exhibit coordinated expression in the renal proximal tubular epithelial cell, J Biol Chem 286 (2011) 19523–19532, https://doi.org/10.1074/jbc.M111.233916.
[27] C. Gebhardt, M. Averbeck, N. Diedenhofen, A. Willenberg, U. Anderegg, J. P. Sleeman, J.C. Simon, Dermal hyaluronan is rapidly reduced by topical treatment with glucocorticoids, J. Invest Dermatol. 130 (2010) 141–149.
[28] K. Briot, C. Roux, Glucocorticoid-induced osteoporosis, RMD Open 1 (2015) e000014.
[29] K.J. Sikes, K. Renner, J. Li, K.J. Grande-Allen, J.P. Connell, V. Cali, R.J. Midura, J. D. Sandy, A. Plaas, V.M. Wang, Knockout of hyaluronan synthase 1, but not 3, impairs formation of the retrocalcaneal bursa, J. Orthop. Res. 36 (2018) 2622–2632, https://doi.org/10.1002/jor.24027.
[30] H. Huang, J. Feng, D. Wismeijer, G. Wu, E.B. Hunziker, Hyaluronic Acid Promotes the Osteogenesis of BMP-2 in an Absorbable Collagen Sponge., Polymers (Basel) 9 (2017). https://doi.org/10.3390/polym9080339.
[31] M. Kawano, W. Ariyoshi, K. Iwanaga, T. Okinaga, M. Habu, I. Yoshioka, K. Tominaga, T. Nishihara, Mechanism involved in enhancement of osteoblast differentiation by hyaluronic acid, Biochem Biophys Res Commun 405 (2011) 575–580, https://doi.org/10.1016/j.bbrc.2011.01.071.
[32] N. Zhao, X. Wang, L. Qin, Z. Guo, D. Li, Effect of molecular weight and concentration of hyaluronan on cell proliferation and osteogenic differentiation in vitro, Biochem Biophys Res Commun 465 (2015) 569–574, https://doi.org/10.1016/j.bbrc.2015.08.061.
[33] Z. Mladenovic, A.-S. Saurel, F. Berenbaum, C. Jacques, Potential role of hyaluronic acid on bone in osteoarthritis: matrix metalloproteinases, aggrecanases, and RANKL expression are partially prevented by hyaluronic acid in interleukin 1-stimulated osteoblasts, J Rheumatol 41 (2014) 945–954, https://doi.org/10.3899/jrheum.130378.
[34] M.I. Alvarez Echazú, O. Perna, C.E. Olivetti, P.E. Antezana, S. Municoy, M. V. Tuttolomondo, J.M. Galdopórpora, G.S. Alvarez, D.G. Olmedo, M.F. Desimone, Recent Advances in Synthetic and Natural Biomaterials-Based Therapy for Bone Defects, Macromol Biosci 22 (2022) e2100383.
[35] A.-K. Picke, J. Salbach-Hirsch, V. Hintze, S. Rother, M. Rauner, C. Kascholke, S. Möller, R. Bernhardt, S. Rammelt, M.T. Pisabarro, G. Ruiz-Gómez, M. Schnabelrauch, M. Schulz-Siegmund, M.C. Hacker, D. Scharnweber, C. Hofbauer, L.C. Hofbauer, Sulfated hyaluronan improves bone regeneration of diabetic rats by binding sclerostin and enhancing osteoblast function, Biomaterials 96 (2016) 11–23, https://doi.org/10.1016/j.biomaterials.2016.04.013.
[36] F. Xing, C. Zhou, D. Hui, C. Du, L. Wu, L. Wang, W. Wang, X. Pu, L. Gu, L. Liu, Z. Xiang, X. Zhang, Hyaluronic acid as a bioactive component for bone tissue regeneration: Fabrication, modification, properties, and biological functions, Nanotechnol Rev 9 (2020) 1059–1079, https://doi.org/10.1515/ntrev-2020-0084.
[37] C. Yang, M. Cao, H. Liu, Y. He, J. Xu, Y. Du, Y. Liu, W. Wang, L. Cui, J. Hu, F. Gao, The high and low molecular weight forms of hyaluronan have distinct effects on CD44 clustering, J Biol Chem 287 (2012) 43094–43107, https://doi.org/10.1074/JBC.M112.349209.
[38] S.A. Freeman, A. Vega, M. Riedl, R.F. Collins, P.P. Ostrowski, E.C. Woods, C. R. Bertozzi, M.I. Tammi, D.S. Lidke, P. Johnson, S. Mayor, K. Jaqaman, S. Grinstein, Transmembrane Pickets Connect Cyto- and Pericellular Skeletons Forming Barriers to Receptor Engagement, Cell 172 (2018) 305–317.e10, https://doi.org/10.1016/j.cell.2017.12.023.
[39] M. Matsushita, H. Kitoh, H. Kaneko, K. Mishima, I. Kadono, N. Ishiguro, G. Nishimura, A novel SOX9 H169Q mutation in a family with overlapping phenotype of mild campomelic dysplasia and small patella syndrome, Am J Med Genet A 161A (2013) 2528–2534, https://doi.org/10.1002/ajmg.a.36134.
[40] A. Heilmann, T. Schinke, R. Bindl, T. Wehner, A. Rapp, M. Haffner-Luntzer, C. Nemitz, A. Liedert, M. Amling, A. Ignatius, The Wnt Serpentine Receptor Frizzled-9 Regulates New Bone Formation in Fracture Healing, PLoS One 8 (2013) e84232.
[41] N. Mitsui, N. Suzuki, M. Maeno, K. Mayahara, M. Yanagisawa, K. Otsuka, N. Shimizu, Optimal compressive force induces bone formation via increasing bone sialoprotein and prostaglandin E2 production appropriately, Life Sci 77 (2005) 3168–3182, https://doi.org/10.1016/j.lfs.2005.03.037.
[42] A. Hoffmann, S. Czichos, C. Kaps, D. Bächner, H. Mayer, Y. Zilberman, G. Turgeman, G. Pelled, G. Gross, D. Gazit, The T-box transcription factor Brachyury mediates cartilage development in mesenchymal stem cell line C3H10T1/2, J Cell Sci 115 (2002) 769–781, https://doi.org/10.1242/jcs.115.4.769.
[43] G. Manickam, P. Moffatt, M. Murshed, Role of SMPD3 during Bone Fracture Healing and Regulation of Its Expression, Mol Cell Biol 39 (2019), https://doi.org/10.1128/MCB.00370-18.
[44] J. Hou, P. Xu, Y. Zhong, Z. Zhou, W. Zhang, Interleukin-21 knockout reduces bone loss in ovariectomized mice by inhibiting osteoclastogenesis, Biosci Biotechnol Biochem 87 (2023) 1265–1273, https://doi.org/10.1093/bbb/zbad103.
[45] C. Nakatomi, M. Nakatomi, T. Matsubara, T. Komori, T. Doi-Inoue, N. Ishimaru, F. Weih, T. Iwamoto, M. Matsuda, S. Kokabu, E. Jimi, Constitutive activation of the alternative NF-κB pathway disturbs endochondral ossification, Bone 121 (2019) 29–41, https://doi.org/10.1016/j.bone.2019.01.002.
[46] S. Yokota, G. Matsumae, T. Shimizu, T. Hasegawa, T. Ebata, D. Takahashi, C. Heguo, Y. Tian, H. Alhasan, M. Takahata, K. Kadoya, M.A. Terkawi, N. Iwasaki, Cardiotrophin Like Cytokine Factor 1 (CLCF1) alleviates bone loss in osteoporosis mouse models by suppressing osteoclast differentiation through activating interferon signaling and repressing the nuclear factor-κB signaling pathway, Bone 153 (2021) 116140, https://doi.org/10.1016/j.bone.2021.116140.
[47] T. Kikuchi, K. Udagawa, Y. Sasazaki, High-molecular-weight Hyaluronan Administration Inhibits Bone Resorption and Promotes Bone Formation in Young-age Osteoporosis Rats, J. Histochem. Cytochem. 72 (2024) 373–385, https://doi.org/10.1369/00221554241255724.
[48] I. Nagaoka, M. Igarashi, K. Sakamoto, Biological Activities of Glucosamine and Its Related Substances, Adv Food Nutr Res. 65 (2012) 337–352, https://doi.org/10.1016/B978-0-12-416003-3.00022-6.
[49] W. Ariyoshi, T. Okinaga, C.B. Knudson, W. Knudson, T. Nishihara, High molecular weight hyaluronic acid regulates osteoclast formation by inhibiting receptor activator of NF-κB ligand through Rho kinase, Osteoarthritis Cartilage 22 (2014) 111–120, https://doi.org/10.1016/j.joca.2013.10.013.
[50] Y. Li, G. Zhong, W. Sun, C. Zhao, P. Zhang, J. Song, D. Zhao, X. Jin, Q. Li, S. Ling, Y. Li, CD44 deficiency inhibits unloading-induced cortical bone loss through downregulation of osteoclast activity, Sci Rep 5 (2015) 16124, https://doi.org/10.1038/srep16124.
[51] E. Pivetta, M. Scapolan, B. Wassermann, A. Steffan, A. Colombatti, P. Spessotto, Blood-derived human osteoclast resorption activity is impaired by Hyaluronan-CD44 engagement via a p38-dependent mechanism, J Cell Physiol 226 (2011) 769–779, https://doi.org/10.1002/jcp.22398.
[52] T.J. de Vries, T. Schoenmaker, W. Beertsen, R. van der Neut, V. Everts, Effect of CD44 deficiency on in vitro and in vivo osteoclast formation, J Cell Biochem 94 (2005) 954–966, https://doi.org/10.1002/jcb.20326.
[53] E.J. Chang, H.J. Kim, J. Ha, H.J. Kim, J. Ryu, K.H. Park, U.H. Kim, Z.H. Lee, H. M. Kim, D.E. Fisher, H.H. Kim, Hyaluronan inhibits osteoclast differentiation via Toll-like receptor 4, J Cell Sci 120 (2007) 166–176, https://doi.org/10.1242/jcs.03310.
[54] W. Ariyoshi, T. Takahashi, T. Kanno, H. Ichimiya, H. Takano, T. Koseki, T. Nishihara, Mechanisms Involved in Enhancement of Osteoclast Formation and Function by Low Molecular Weight Hyaluronic Acid, J. Biol. Chem. 280 (2005) 18967–18972, https://doi.org/10.1074/jbc.M412740200.
[55] L. Pan, H. She, Y. Hu, L. Liu, H. Wang, L. Zhu, Toll-like receptor 4 deficiency affects the balance of osteoclastogenesis and osteoblastogenesis in periodontitis, Int Immunopharmacol 137 (2024) 112500, https://doi.org/10.1016/j.intimp.2024.112500.
[56] C.W. Lee, J.Y. Seo, J.W. Choi, J. Lee, J.W. Park, J.Y. Lee, K.-Y. Hwang, Y.S. Park, Y., Il Park, Potential anti-osteoporotic activity of low-molecular weight hyaluronan by attenuation of osteoclast cell differentiation and function in vitro, Biochem Biophys Res Commun 449 (2014) 438–443, https://doi.org/10.1016/j.bbrc.2014.05.050.
[57] J. Sapudom, K.-T. Nguyen, S. Martin, T. Wippold, S. Möller, M. Schnabelrauch, U. Anderegg, T. Pompe, Biomimetic tissue models reveal the role of hyaluronan in

melanoma proliferation and invasion, Biomater Sci 8 (2020) 1405–1417, https://doi.org/10.1039/C9BM01636H.
[58] D.W. Dempster, J.E. Compston, M.K. Drezner, F.H. Glorieux, J.A. Kanis, H. Malluche, P.J. Meunier, S.M. Ott, R.R. Recker, A.M. Parfitt, Standardized nomenclature, symbols, and units for bone histomorphometry: a 2012 update of the report of the ASBMR Histomorphometry Nomenclature Committee, J Bone Miner Res 28 (2013) 2–17, https://doi.org/10.1002/jbmr.1805.
[59] A.-K. Picke, G.M. Campbell, M. Blüher, U. Krügel, F.N. Schmidt, E. Tsourdi, M. Winzer, M. Rauner, V. Vukicevic, B. Busse, J. Salbach-Hirsch, J.P. Tuckermann, J.C. Simon, U. Anderegg, L.C. Hofbauer, A. Saalbach, Thy-1 (CD90) promotes bone formation and protects against obesity, Sci Transl Med 10 (2018), https://doi.org/10.1126/scitranslmed.aao6806.
[60] S. Chen, Y. Zhou, Y. Chen, J. Gu, fastp: an ultra-fast all-in-one FASTQ preprocessor, Bioinformatics 34 (2018) i884–i890, https://doi.org/10.1093/bioinformatics/bty560.
[61] D. Kim, B. Langmead, S.L. Salzberg, HISAT: a fast spliced aligner with low memory requirements, Nat Methods 12 (2015) 357–360, https://doi.org/10.1038/nmeth.3317.
[62] M. Pertea, D. Kim, G.M. Pertea, J.T. Leek, S.L. Salzberg, Transcript-level expression analysis of RNA-seq experiments with HISAT, StringTie and Ballgown, Nat Protoc 11 (2016) 1650–1667, https://doi.org/10.1038/nprot.2016.095.
[63] M.I. Love, W. Huber, S. Anders, Moderated estimation of fold change and dispersion for RNA-seq data with DESeq2, Genome Biol 15 (2014) 550, https://doi.org/10.1186/s13059-014-0550-8.
[64] M. Ashburner, C.A. Ball, J.A. Blake, D. Botstein, H. Butler, J.M. Cherry, A.P. Davis, K. Dolinski, S.S. Dwight, J.T. Eppig, M.A. Harris, D.P. Hill, L. Issel-Tarver, A. Kasarskis, S. Lewis, J.C. Matese, J.E. Richardson, M. Ringwald, G.M. Rubin, G. Sherlock, Gene Ontology: tool for the unification of biology, Nat Genet 25 (2000) 25–29, https://doi.org/10.1038/75556.
[65] S. Carbon, E. Douglass, B.M. Good, D.R. Unni, N.L. Harris, C.J. Mungall, S. Basu, R. L. Chisholm, R.J. Dodson, E. Hartline, P. Fey, P.D. Thomas, L.-P. Albou, D. Ebert, M.J. Kesling, H. Mi, A. Muruganujan, X. Huang, T. Mushayahama, S.A. LaBonte, D. A. Siegele, G. Antonazzo, H. Attrill, N.H. Brown, P. Garapati, S.J. Marygold, V. Trovisco, G. dos Santos, K. Falls, C. Tabone, P. Zhou, J.L. Goodman, V. B. Strelets, J. Thurmond, P. Garmiri, R. Ishtiaq, M. Rodríguez-López, M.L. Acencio, M. Kuiper, A. Lægreid, C. Logie, R.C. Lovering, B. Kramarz, S.C.C. Saverimuttu, S. M. Pinheiro, H. Gunn, R. Su, K.E. Thurlow, M. Chibucos, M. Giglio, S. Nadendla, J. Munro, R. Jackson, M.J. Duesbury, N. Del-Toro, B.H.M. Meldal, K. Paneerselvam, L. Perfetto, P. Porras, S. Orchard, A. Shrivastava, H.-Y. Chang, R. D. Finn, A.L. Mitchell, N.D. Rawlings, L. Richardson, A. Sangrador-Vegas, J. A. Blake, K.R. Christie, M.E. Dolan, H.J. Drabkin, D.P. Hill, L. Ni, D.M. Sitnikov, M. A. Harris, S.G. Oliver, K. Rutherford, V. Wood, J. Hayles, J. Bähler, E.R. Bolton, J. L. De Pons, M.R. Dwinell, G.T. Hayman, M.L. Kaldunski, A.E. Kwitek, S.J. F. Laulederkind, C. Plasterer, M.A. Tutaj, M. Vedi, S.-J. Wang, P. D'Eustachio, L. Matthews, J.P. Balhoff, S.A. Aleksander, M.J. Alexander, J.M. Cherry, S.R. Engel, F. Gondwe, K. Karra, S.R. Miyasato, R.S. Nash, M. Simison, M.S. Skrzypek, S. Weng, E.D. Wong, M. Feuermann, P. Gaudet, A. Morgat, E. Bakker, T.Z. Berardini, L. Reiser, S. Subramaniam, E. Huala, C.N. Arighi, A. Auchincloss, K. Axelsen, G. Argoud-Puy, A. Bateman, M.-C. Blatter, E. Boutet, E. Bowler, L. Breuza, A. Bridge, R. Britto, H. Bye-A-Jee, C.C. Casas, E. Coudert, P. Denny, A. Estreicher, M.L. Famiglietti, G. Georghiou, A. Gos, N. Gruaz-Gumowski, E. Hatton-Ellis, C. Hulo, A. Ignatchenko, F. Jungo, K. Laiho, P. Le Mercier, D. Lieberherr, A. Lock, Y. Lussi, A. MacDougall, M. Magrane, M.J. Martin, P. Masson, D.A. Natale, N. Hyka-Nouspikel, S. Orchard, I. Pedruzzi, L. Pourcel, S. Poux, S. Pundir, C. Rivoire, E. Speretta, S. Sundaram, N. Tyagi, K. Warner, R. Zaru, C.H. Wu, A. D. Diehl, J.N. Chan, C. Grove, R.Y.N. Lee, H.-M. Muller, D. Raciti, K. Van Auken, P. W. Sternberg, M. Berriman, M. Paulini, K. Howe, S. Gao, A. Wright, L. Stein, D. G. Howe, S. Toro, M. Westerfield, P. Jaiswal, L. Cooper, J. Elser, The Gene Ontology resource: enriching a GOld mine, Nucleic Acids Res 49 (2021) D325–D334, https://doi.org/10.1093/nar/gkaa1113.